ABSTRACT

ZHU, SHAN. Multi-Dimensional Colloidal Assembly in External Fields. (Under the direction of Orlin D. Velev).

Use of external fields to drive assembly processes is able to induce tailored, long-range inter-particle forces with tunable intensity and directionality that can generate highly ordered and programmable multi-dimensional structures. We employ two methods to achieve unique multi-dimensional colloidal assembly, one involving multi-directional interaction resulting from induced dipole interaction in AC electric field and the other including both electric and magnetic fields in 2D experimental plane.

While much effort has been devoted to exploring the assembly of spherical colloids, few reports have been focused on the directed assembly of non-spherical particles with Janus or patchy morphologies. Here, we use photolithographic techniques to fabricate a wide range of anisotropically shaped patchy particles and follow their assembly in liquid suspensions under the influence of dielectrophoresis (DEP) in a novel inverse experimental setup. We analyze specifically the assembly of one-side coated cubic particles across a range of field parameters, and report distinct, well-ordered assembly architectures. By using numerical simulations to model the field interactions between these particles, we interpret the results of the assembly process and explain how they can be controlled by the position of the metal facet, the intensity and frequency of alternative current. The resulting structures, and similar ones produced through the field-directed assembly of patchy anisotropic particles, can possess unique electrical and optical properties and may have potential applications in a

number of future technology applications such as microactuators, metamaterials and multiferroic materials.

As fabrication of patchy particles take time and much work, the idea of assembling a bi-responsive 2D percolation based on non-patchy spherical particles by combing different type of external fields and placing them multi-dimensionally is very convincing. Using the design where AC electric field and magnetic field are positioned perpendicular to each other, we are able to percolate chains formed by dielectric particles and magnetic particles in direction of fields respectively. Two mechanism ‘competitive assembly’ and ‘re-assembly’ based on the order of two fields are analyzed kinetically and statically, in order to achieve well percolated network with low particle number density. To simplify the characterization, computer programming is designed to get much more detailed information about particle interaction, for better understanding the 2D network. The architectures we get may find potential application as material with anisotropy in electric and magnetic conductivity or low density gels.

Multi-Dimensional Colloidal Assembly in External Fields

by
Shan Zhu

A thesis submitted to the Graduate Faculty of
North Carolina State University
in partial fulfillment of the
requirements for the degree of
Master of Science

Chemical Engineering

Raleigh, North Carolina

2013

APPROVED BY:

_____	_____
Michael Dickey	Saad A. Khan

_____
Orlin D. Velev
Chair of Advisory Committee

DEDICATION

To my husband, Tianxiang Gao, who is my love and source of refuge along completing my master study.

To my coming baby, my parents and parents in law.

BIOGRAPHY

Shan Zhu was born in 1988 in a city on the east coast of China, Qingdao. From ages sixteen to nineteen she attended the top high school in Qingdao, Qingdao No.2 middle school. She was enrolled by Zhejiang University in 2007, which is one of the top universities in China, without college entrance test because of her excellent performance during high school. In 2011, she worked in University of California, Davis as Junior Research Specialist for half-year. After finishing her Bachelor Degree in Zhejiang University, she was enrolled in North Carolina State University in 2011 for a PhD program in Chemical Engineering. Since 2012 she was working under the guidance of Dr. Orlin D. Velev.

Besides the academic careers, Shan Zhu is very enthusiastic with her life. She loves sports and music, and she would always like to try new things. Shan Zhu is also a person with great responsibility and love for her family. She found her love in North Carolina during year 2012 when she first met Tianxiang Gao, her husband who is pursuing a doctoral degree in University of North Carolina at Chapel Hill. Both of them studied in the same high school and undergraduate university, but they never knew each other until they met in North Carolina. They got married with their serendipity in January of 2013. In July, they got great news of Shan's pregnancy. The coming of the new baby will bring great pleasure for them.

ACKNOWLEDGMENTS

I could not have accomplished this thesis without the help and support of my family, friends and colleagues. However, with his wisdom, guidance and enthusiasm, my adviser Dr. Orlin D. Velev has played the main role in this work. His positive and energetic personality has always kept me on track. He has been available for me all the time no matter how busy his schedule is. I am really lucky to have worked with him and to have been a part of Velev Research Group.

I would like to thank the members of my committee, Dr. Michael Dickey, Dr. Saad A. Khan, and Dr. Orlin D. Velev for their time and constructive feedbacks. I would like to acknowledge all the CBE faculty members and staff for their favors. Also I am grateful for the financial support and precious fellow experience of Triangle Material Research Science and Engineering Center (MRSEC) in addition to CBE department.

Throughout my graduate years I have had great colleagues and friends. I would like to thank my fellow doctoral students—those who have moved on, those who are about to see the end, and those just beginning—for their support, feedback, and friendship. I would like to thank each, Stoyan, Liz, Jairus, Etienne, Elena, Daniel, Alex, Tian, Yan, Naren, Rachita, Selver, Anne-Laure, Bhuvnesh, Tim, Stephanie and Brittany for their assistance, discussions and friendship. Also I would like to thank gratefully my postdoc mentor Bhuvnesh Bharti for the great advice and support in all perspectives, and collaborators Wyatt Shields (Duke) and Dr. Lopez Gabriel for working together closely. Last, but certainly not least, there are no words to describe my appreciation for husband's motivation and support.

TABLE OF CONTENTS

LIST OF FIGURES

Chapter 1
Introduction

Colloidal assembly has attracted vast interest among scientists all over the world in the last couple decades. Due to their unique properties, such as high surface-to-volume ratio, long-range ordering and large packing density, colloidal particle assemblies can find potential applications in various areas. For example, they can produce porous materials and be used as photonic crystals and biosensors.[1-4] Common techniques of colloidal assembly include evaporation of medium, use of external field, absorption and others, among which the assembly assisted by external field (AC electric/magnetic/acoustic) draws much attention recently and is undergoing wide investigation.[5-9] Though approaches, such as maximization of entropy,[10] sedimentation,[11,12] and dehydration,[13, 14] provide various ways of assembling ordered structures, they were mostly limited to producing multidimensional close-packed geometries due to lack of intrinsic mechanism of particle alignment. However, the use of external fields to drive assembly processes is able to induce tailored, long-range inter-particle forces with tunable intensity and directionality that can generate uniform and programmable structures.[5, 8] Dielectrophoresis (DEP) and magnetophoresis (MAP) are two common methods used in directed assembly that introduce orientation-dependent interactions between multi-component patchy particles. DEP has been used to concentrate particles for crystallization by moving charged or uncharged particles along the gradient of an AC electric field, while a similar mechanism has been demonstrated for MAP assembly of crystals from magnetic particles.[7, 15]

1.1 Background and goal of dielectrophoretic assembly

Compared to DC electric field, where electrophoretic motion of particles occurs with the background electro-osmotic flows of the liquid, AC electric field reduces the complication in the experimental implementation by avoiding electro-osmotic drift. The forces that the AC electric fields exert on particles include dielectrophoresis and particle chaining. They can be

efficiently controlled by adjusting field parameters such as magnitude, frequency, wave shape, wave symmetry, and phase. [16-19]

The origin of the AC effects is the frequency-dependent polarization of particles in AC fields applied across particle suspension. The sign and magnitude of the dipoles induced in the particles are given by the real part of the Clausius–Mossotti function, K

$$Re\left|\underline{K}\right| = \frac{\varepsilon_2-\varepsilon_1}{\varepsilon_2+2\varepsilon_1} + \frac{3(\varepsilon_1\sigma_2-\varepsilon_2\sigma_1)}{\tau_{MW}(\sigma_2+2\sigma_1)^2(1+\omega^2\tau_{MW}^2)} \quad (1)$$

$$\tau_{MW} = \frac{\varepsilon_2+2\varepsilon_1}{\sigma_2+2\sigma_1} \quad (2)$$

where ω is the angular frequency of the field, ε_1 and σ_1 are the dielectric permittivity and conductivity of the media, while ε_2 and σ_2 are those of the particles.[19] Metallic and highly conductive particles are always strongly polarized (with positive $\left|\underline{K}\right|$) at most AC field frequencies. Dielectric particles whose bulk permittivity is lower than the water media, such as polystyrene microspheres, exhibit higher polarizability at low frequencies (positive DEP), while performing negative DEP behavior at high frequencies. The dielectrophoretic force, $\vec{F}_{DEP}$, based on the interaction of induced dipoles on spherical particles within a non-uniform AC electric field, is

$$\vec{F}_{DEP} = 2\pi\varepsilon_1 Re\left|\underline{K}\right| r^3 \nabla E^2 \quad (3)$$

where r is the radius of particles and ∇E^2 is the gradient of electric field squared. Positive DEP pulls particles along the gradient into the areas of highest field intensities, while particles are pushed away from areas with negative DEP.[16, 19] Interactions between induced dipoles on spherical particles along the direction of the electric field are described by

$$F_{chain} = -C\pi\varepsilon_1 K^2 E^2 \quad (4)$$

where the coefficient C ranges from 3 to >10^3 depending on the distance between the particles and the length of the particle chain.[7, 17] Notably, the chaining force acting on particles of similar electrical properties is always positive and attractive.

Previous studies focused mainly on spherical particles with or without anisotropic metal

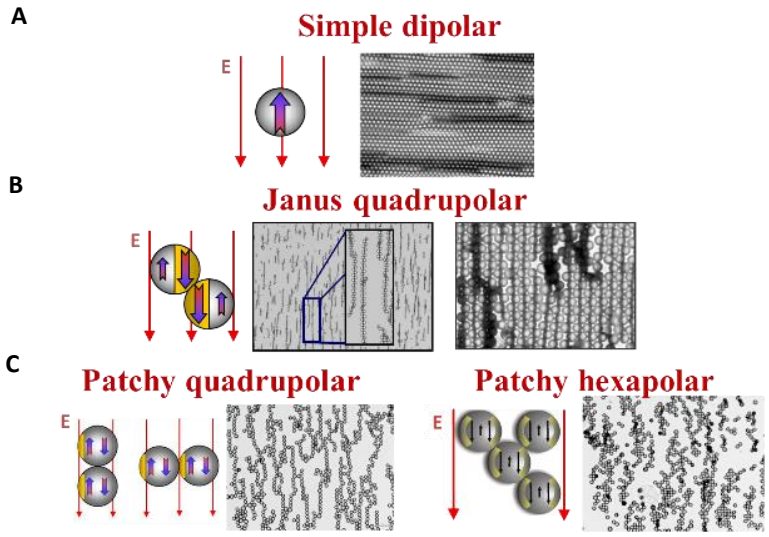

Figure 1. Examples of various 2D structures formed by spherical particles by DEP involving different types of dipolar interaction. (A) 2D crystals formed by latex particles, [7] (B) staggered chains of Janus particles, [8] (C) programmable structures formed by two types of patchy particles. [20]

coating.[7, 8, 20] Simple dipolar interaction among isotropic latex or silicon microspheres lead to close-packed hexagonal geometric crystals in 2D or 3D depending on the number density of particle suspension.[7,8] For metal-coated spherical particles, the assembled structures were dependent strongly on type of metal patch.[8, 20] Janus particles, synthesized by coating gold on polystyrene microspheres to yield 50% coverage of surface area, have different properties of each half. [8, 20-23] The dielectrophoretic response of the metallodielectric Janus particles depended strongly on the frequency and intensity of the applied field.[8] Low frequency (0.1~10kHz) AC electric fields resulted in unbalanced liquid flows and nonlinear, induced-charge electrophoretic motion of the particles in direction perpendicular to the field,[6,8] while particles subjected to high frequency of the field could

form staggered chains due to quadrupolar interaction where strong polarizability of metal played an essential role.[8] Two types of patchy microspheres were also studied and interesting structures were found in the experiments.[20] One type of particle had a single metal patch covering 11% of the total dielectric latex particle surface, and the induced dipoles in gold patch and the polystyrene core of similar magnitude but in the opposite direction resulted in alignment in two directions perpendicular to each other. The other type of particle had two independent metal patches (each covering estimated 25% of the total surface area) on opposite poles, and diagonal chains have been at 45^0 to the field.[20] (Figure 1) With anisotropy in polarizability of particle based on metal patches, promising structures with unique geometries were achieved and its fundamental principle of polar interaction were understood and interpreted.

In our study, we have focused on even more complex DEP assembly of particles with anisotropy both in polarizability and particularly in shape. As deep exploration has already been done for spherical particles, we sought to understand how shape combined with metal coating of particle may perform in the DEP setting. Initial attempt of dielectrophoretic assembly of non-spherical particles has been done for various shapes, such as hexnut, rod, disc, and "boomerang". [24] Chaining and packing have been observed for each specific shape design accordingly, while less explanation of fundamentals was included. What's more, particles used were not metal-coated, therefore polarizability all over the particles was uniform, though the shapes of particles were non-spherical and irregular. In addition, when the shape is taken into consideration, Eqn. 1-4 derived for the specifically spherical particles need to be modified based on the geometric shape of particles, which would could be difficult because of the need for integration over the 3D geometry. In this case, simulation would possibly better serve to understand the system.

In short, our goal is to further understand the DEP assembly of the complex particles with non-spherical shape and anisotropic metal coating in attempt to producing potential materials with anisotropic physical properties (conductivity, transparency, etc.).

1.2 Background and goal of producing 2D percolated network in electric and magnetic fields

So far, with dielectrophretic assembly, as mentioned above, the AC electric field can be used for assembly of a variety of 2D structures based on spherical particles by modification of

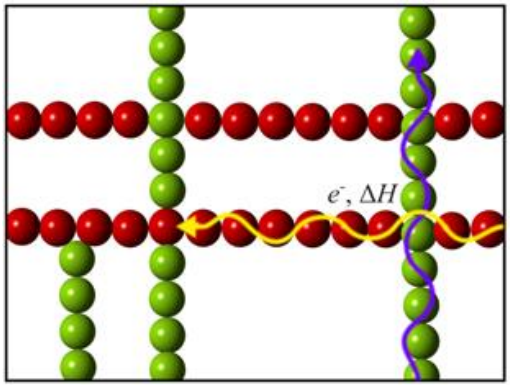

Figure 2. Proposed 2D percolated network by AC and magnetic fields perpendicular to each other.

particle surface with designed metal patching. However, the acquisition of patchy particles required the fabrication process to be precise and accurate, which made it difficult and time-consuming. [8, 9] Can we achieve 2D structures in a simpler way? An idea came up for including the action of a magnetic field in addition to the AC electric field. Since both fields have the capability of orienting isotropic particles in the direction of each field, combination of DEP/MAP could create chaining in 2D by placing the fields with certain angle in the plane of the particle suspension.

Similar to the DEP, MAP can induce magnetic dipoles for magnetically polarizable particles responding to the magnetic field and attractive dipole-dipole interaction lead to chains along the direction of field. The magnetophoretic force is

$$\vec{F}_{MAP} = \rho V \nabla(\vec{M}_0 \cdot \vec{B} + \frac{V\chi}{\mu_0}(\vec{B} \cdot \nabla)\vec{B} \quad (5)$$

$$\vec{H} = \vec{B}/\mu \quad (6)$$

where ρ and V are density and volume of particle, $\vec{M}_0$ and μ_0 are initial magnetization and permittivity of free space, $\vec{B}$ is magnetic induction, χ is susceptibility and $\vec{H}$ is magnetic field. MAP assembly techniques are tuned in a similar manner by adjusting the field magnitude and the type of carrier fluid, leading to a corollary set of structures to those produced by DEP technique. [25-28]

Percolation has been understood to some extent from the perspective of numerical simulation for colloidal, polymer, and other kinds of systems. [29-30] However, the creation of such network practically has been barely studied. The novel idea of combination of two types of fields under the same experimental setupprovides possibility of achieving this by a novel technique.

Our goal here is to achieve assembly of two-directionally percolated particle networks using orthogonal electric and magnetic fields. The percolated network may find potential application as material with anisotropy in electric and magnetic conductivity or low density gel.

Chapter 2
Dielectrophoretic assembly of complex particles

2.1 Materials & fabrication

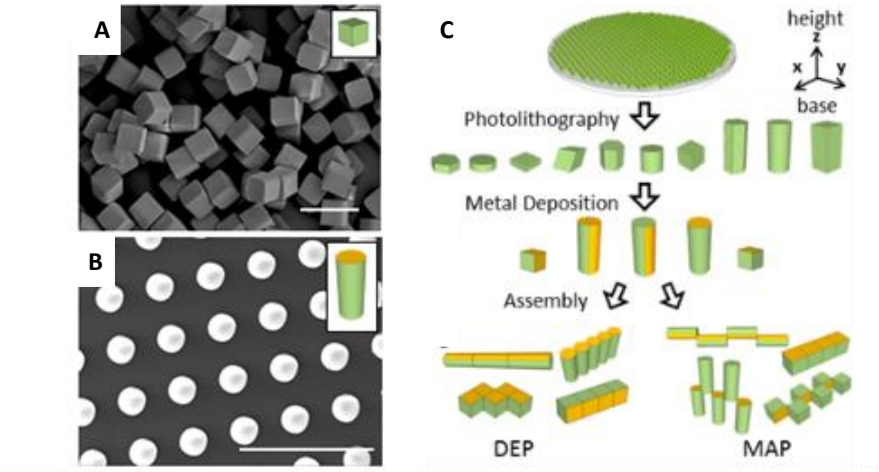

Figure 3. Fabrication of non-spherical particles with metal coating. (A) SEM images of 10 μm SU-8 cubes, (B) 25 μm tall cylinders top-coated with 15 nm Cr and 50 nm Au before removal from the silicon wafer substrate, (C) schematic depicting the steps in the fabrication and assembly of anisotropic patchy particles. [31]

The metal-coated particles with anisotropy both in shape and in polarizability were fabricated via photolithography after which metal evaporation was used to pattern bare particles.

SU-8 negative photoresist (MicroChem, Newton, MA) was used to as base material for fabrication in favor of its ability to generate large aspect ratio structures. Following the protocols provided by MicroChem (MicroChem, Inc., Newton, MA), SU-8 was spin-coated onto silicon wafers (Addison Engineering, Inc., San Jose, CA) with precise thicknesses. Photomasks (Photo Science, Inc., Torrance, CA) then were used to pattern SU-8 with shapes (cubes, cylinders, or hexagons) of 5 to 10 μm in size with equal spacing. After exposure to UV light (365 nm, 120 – 250 mJ cm^{-2}, Suss MicroTec MA6/BA6, Garching, Germany), spin

coated wafers were post-baked, developed and rinsed with isopropyl alcohol and dreied in nitrogen. [31]

To achieve the anisotropy in polarizability, metal layers were deposited on the particles by Electron Beam Metal Evaporator (EBME) (CHA Industries Solution E-Beam, Fremont, CA). Patchy particles were made by coating with 15 nm Cr followed by 50 nm Au, and different types of coating, such as top, angle (adjacent two sides), and side, were well achieved. Specially, the angle-deposited coating was enabled by tilting the stage of bare cubes to angles near 45^0, while for cylindrical particles, removal and suspension of particles from wafers in water together with natural evaporation helped sedimentation where side of cylinders faced up, thus side coating can be well performed by EBME. [31]

Particles after fabrication were suspended in 0.1 vol. % Tween 20 (Sigma-Aldrich, St. Louise, MO) solution to reduce possible aggregation from their particle sticking and physical contact due to sedimentation at the bottom of container. Metal coated particles were mixed well and sonicated before every experiment to guarantee that they were dispersed uniformly.

2.2 Design of experimental setup using inverse cell

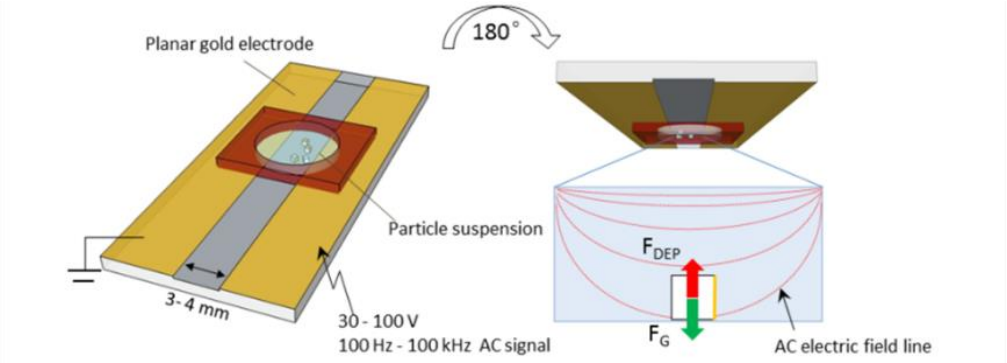

Figure 4. Schematic of the inverted DEP assembly configuration. The DEP assembly cell is loaded, inverted, and then excited in an AC electric field with a gradient oriented against the direction of gravity. [31]

The experimental cell consisted of microscope grass chip where the co-planar metal (15 nm Cr and 100 nm Au) electrodes with 3 mm gap were deposited. Imaging chamber (Grace Bio-Labs Inc, Bend, OR) with 20 mm inside diameter and 0.6 mm depth was filled with particle

suspension and attached onto the electrodes where AC signal (~ 30 – 100 V, 100 Hz – 100kHz) was switched on. [31] Using the same design with previous studies for small microspheres [7, 8, 20] where the chamber was placed above electrodes, the cubic and cylindrical particles without metal coating demonstrate precise chaining along the direction of field. In agreement with dielectrophoretic fundamentals, bare particles without anisotropy in polarizability aligned in the way such that the maximum dipoles among their dimension 'connected' head to toe. As shown in Figure 5, cylinders (height = 25 μm, dia. = 10 μm) formed long chains along the dimension of height, while the cubes aligned isotropically with their left or right sides pointing from the plane of view. This normal design worked well for non-coated particles as well.

However, in the experiments, the metal coated particles didn't show distinct structures if we placed the chamber on top of the electrodes. Since metal has much larger polarizability

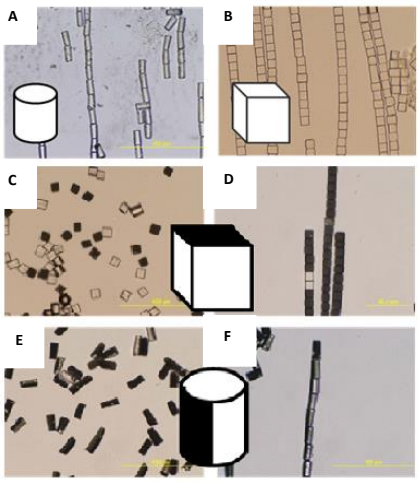

Figure 5. Optical micrographs of DEP assemblies of cubes and cylinders. (A) chains of bare cylinders in normal cell, (B) chains of bare cubes in normal cell, (C) one-side coated cubes without field, (D) one-side coated cubes in inverse cell, (E) side coated cylinders without field, (F) side coated cylinders in inverse cell.

compared with particle polymer SU-8 and positive dielectrophoresis tends to drag these particles to the highest field intensity, it should play the significant role of orienting particles in the field. But in a normal cell, particles initially placed randomly faced obstacle to rotate

or flip over to their preferential orientation, because both the gravity and dielectrophoretic force by co-planar electrodes onto the particles were in the same direction pointing down to the bottom. The relatively large size compared with microspheres in previous experiments and edges of cubes contributed to arrested motion. Therefore, the structure formed in normal cell for metal coated particles depended more on the initial placement whether the metal was on top/bottom or on the side.

To apply the experimental setup for non-spherical metal coated particles, innovation was made by inverting the normal cell 180^0, so that the dielectrophoretic force now pulls in the direction opposite to the gravity offered the capability for particles to be lifted and rotate. Figure 5 shows how one-side coated cubes and side coated cylinders aligned in the new inverted experimental design. One-side coated cubes, appeared transparent when the metallic patch was on one of the sides (not in the viewing plane) of particles, whereas they appeared opaque when the metal was on the top or bottom of the particles within the viewing plane. Side-coated cylinder particles appeared darker, as the transparent SU-8 allowed the light transmission reflecting half side of metal. Regardless of their initial position, metal coated particles formed uniform structures within the inverse experimental cell.

2.3 Configurations of one-side coated cubes under various conditions

Among variety of shape and metal coating, our study initially focused on one-side coated cubes which seemed to be less complicated. It is shown by Figure 6 that the manipulation of

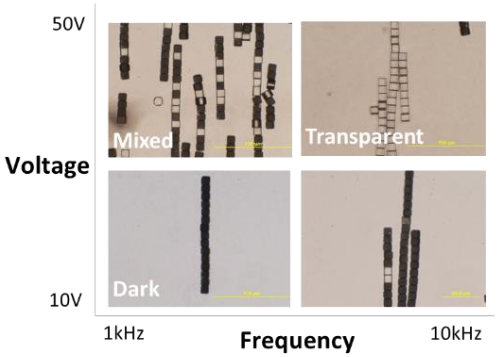

Figure 6. Diagram of configurations formed by one-side coated cubes depending on the voltage as well as frequency of the field.

the AC electric field strength and frequency provide the two main parameters to tailor the assembly.

At relatively low volume fraction, the one-side coated cubes, they form different configurations as a function of field strength and frequency. At low frequency (1 kHz – 10 kHz) and low voltage (10 V- 30 V), dark configuration where metal is on the top or bottom predominated. Subjected to the field, single, isolated dark particles oriented at an angle of 45^0 in the viewing plane with respect to the field. This diagonal orientation prevails because the maximum dipole (diagonal between opposite corners) in the field direction is induced across the metal coating. The transparent particles either rolled over to appear dark before getting contact with other particles or aligned with others first then flipped over. As particles were attracted toward each other by dipole-dipole interaction, they reoriented and aligned, such that their edges were parallel and orthogonal to the field direction. They didn't form rhombic asymmetry where all particles oriented at an angle of 45^0 with regard to the field direction, since there is torque τ exerted on the particles when they are at an angle to the field. The toque is proportional to the size of the particle (a^3), square of field intensity (E^2) and angle to the field direction (θ). [19] As the equation below shows, the maximum toque will be exerted if the angle is 45^0.

$$\tau \propto a^3 E^2 \cos 2\theta \qquad (7)$$

When more and more particles came together, they organized into dark chains along the direction of field.

When we increased the voltage at frequencies lower than 10 kHz, the configuration became less uniform for there was no favorable orientation. Dark and transparent particles seemed to assemble randomly, suggesting the field strength was sufficient to induce chaining prior to reorientation. These mixed structures existed under two kinds of circumstances. One occurred at very low frequency and relatively high voltage, while the other happened when the volume fraction of the particle suspension was quite large. Both lead to mixed configuration because of rapid assembly and strong attraction of particles, where kinetically

trapping happened. It is essential and the reason why we kept on doing the experiments at low volume fraction of suspension.

In contrast, at high voltage and high frequency (≥ 10 kHz), the transparent configuration became predominant. It's hard to tell which side of metal stays for the transparent particles in the microscopic image, but it is clear that the metal is on one of possible four sides of the square at the plane of view. Once field was turned on, the randomly placed isolated transparent particles rotated to their preferential position with edges parallel or perpendicular the field direction, by which the maximum dipole induced in the metal coating aligned in the same direction of field. Meantime, the dark particles rolled over to transparent appearance during the assembly. Chaining based on dipole-dipole attraction became faster at higher voltage, which is expected. If assembly was achieved by forming dark chains at low voltage and switching to high voltage, the dark chains then rolled over simultaneously. It's always exciting to see particles in vision changing from dark to bright. In addition, at even higher frequency, the required voltage for the configuration changing became lower.

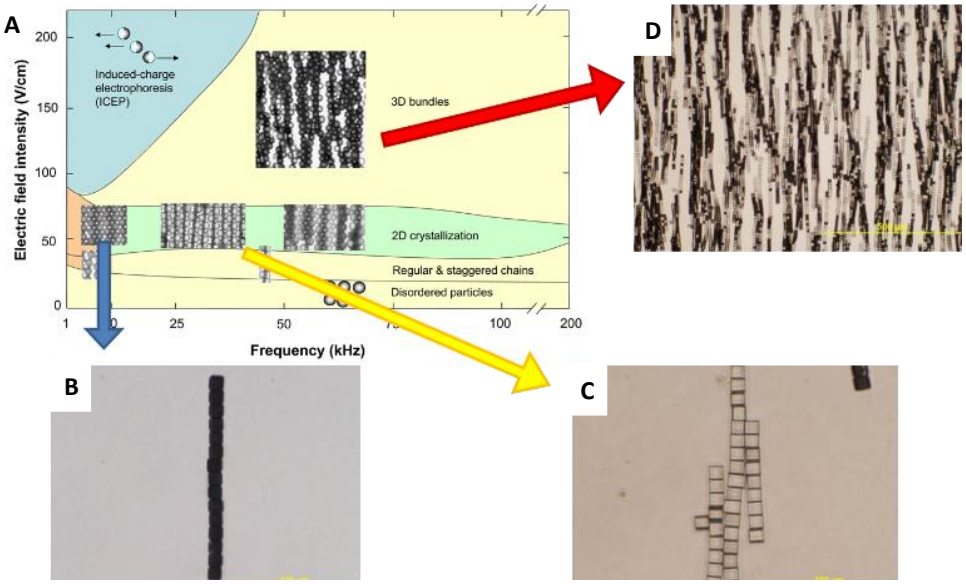

Figure 7. Analogy of one-side coated cubes to Janus particles in AC field. (A) phase diagram of Janus particles corresponding to intensity and frequency of the field, [8] (B) dark configuration of one-side coated cubes, (C) transparent configuration of one-side coated cubes, (D) 3D bundles formed by one-side coated cubes.

In short, we achieved turning the assembly of one-side coated particles into well uniform process of making distinctive structures by manipulating the frequency and voltage of the field. It agreed with the fundamental of dielectrophoresis and is in line with what was previously reported for Janus microspheres [8, 32]. We found similarity with analogic polar interaction between two systems. But from the perspective of potential application, one-side coated cubes could be more meaningful, as their physical properties (heat/electric conductivity, transparency) are anisotropic, which might be useful in the making of novel material.

2.4 Characterization of the system

To verify the existence of various stable configuration, we employed statistical analysis. By

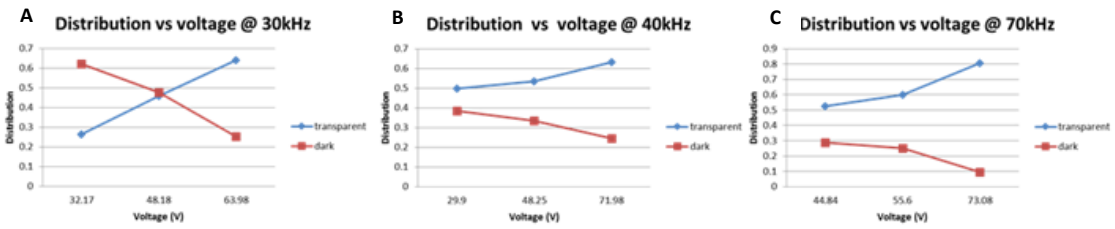

Figure 8. Distribution of dark and transparent particle orientation versus voltage at various frequencies of field. (A) 30 kHz, (B) 40 kHz, (C) 70 kHz.

counting the number of two kinds of particles, the distribution of dark and transparent particle orientation was calculated and evaluated at frequencies and low to high voltage. Figure 8 illustrated the same trend as mentioned above: at frequency larger than 10 kHz, the dark still prevailed if the voltage was low, but with increase of voltage the transparent configuration became dominating; as frequency went higher, the voltage needed for configuration transition was lower. However, during this process, we observed some interesting sedimentation phenomena of these one-side coated cubes, where shaking and re-dispersion between experiments resulted in more dark particles thus not random placement at initial. To better represent the influence of electric field, we improved by taking into account the initial particle distribution and calculated how many particles transited to the other

configuration. An example is shown in Figure 9, the conclusion is still that high voltage favors the transparent configuration, while at low voltage small amount of initial transparent

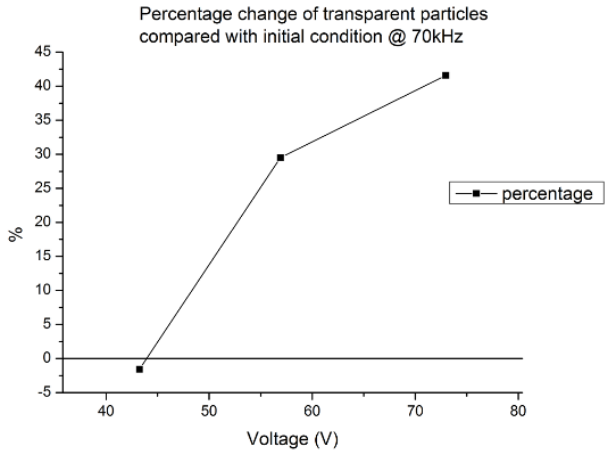

Figure 9. Percentage change of transparent particles compared with initial condition at 70 kHz.

particles turned into dark orientation at 70 kHz, (Figure 9).

To understand the formation of two different configurations, we used numerical simulation. For the transparent configuration, COMSOL simulation was used to predict the most likely orientation of the particles as well as the kinetics during the particle-particle interaction. In the 2D simulation, the complex permittivity ($\tilde{\varepsilon}$) was calculated for four domain components in the system including thin conductive counter-ionic layer around the particle, gold layer, SU-8 core, and water media. With calculation of electric distribution by Laplace equation

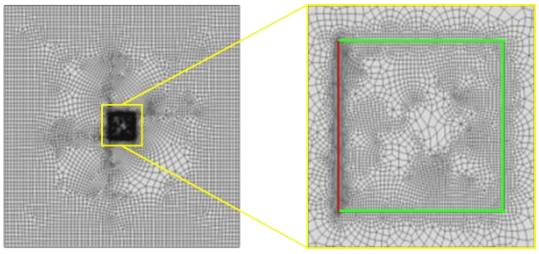

Figure 10. Example of meshing of single one-side coated cube in AC field.

(Eqn. 9) and local electric energy based on result of Eqn. 9 (Eqn. 10), the overall energy of the system (Eqn. 11) was got by integration over the volume. [8]

$$\tilde{\varepsilon} = \varepsilon_0 \varepsilon_r - \frac{i(\sigma)}{\omega} \quad (8)$$

$$\Delta^2 \varphi = 0 \quad (9)$$

$$w_{es} = \frac{1}{2} DE = \frac{1}{2} \varepsilon_0 E^2 \quad (10)$$

$$W_e = \int_V w_{es} dV \quad (11)$$

The numerical modeling over a range of frequencies shows that at low frequencies (<10 kHz) both the metallic coatings and the counterionic layers around the SU-8 facets have greater

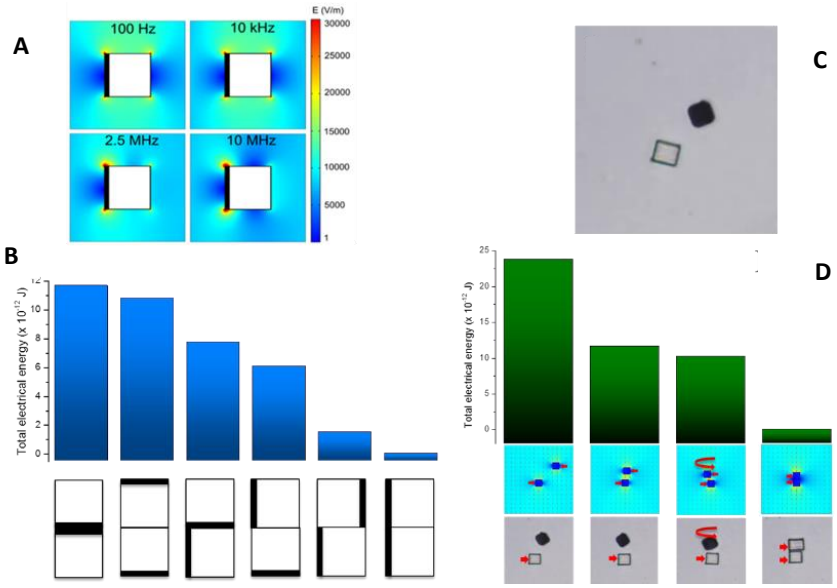

Figure 11. COMSOL simulation of one-side coated cubes in AC field. (A) distribution of electric energy of single particles under different frequencies, [31] (B) total electric energy of six possible configurations of two adjacent transparent particles,[31] (C) a dark particle approaching a transparent one, (D) electric energy during the process of dark particle approaching a transparent one.

electrical polarizability than the aqueous medium surrounding them. Thus the particle has features qualitatively similar to a point dipole. At higher frequencies, the ionic mobility hardly plays a role and SU-8 becomes less polarizable than water, such that the field of the

composite structure resembles a quadrupole (Figure 11A, 10 MHz). The result of this numerical simulation agrees with results of Janus particle [8] and the analogy again draws attention to the similar dielectrophoretic behavior for particles with different shapes and in different experimental cells. One main reason for employing COMSOL simulation is to predict the precise configuration of transparent particles at high frequency and voltage, as from the microscopic image, the 65 nm metal coating is not visible, given the resolution of camera and magnification of microscope. The electrical energies of six possible configurations of a couple of transparent particles were calculated (Figure 11B). When both metallic faces were in parallel to the field and on the same side of the cube, the total energy was minimized. If the metallic faces parallel to the field but on different sides, the energy was the second lowest. These two cases were more likely to occur in real system compared with other four where at least one metal face was perpendicular to the direction of the field.

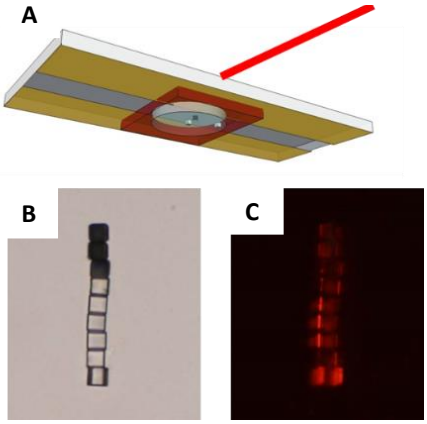

Figure 12. Laser check of metal side of transparent particles. (A) schematics of shining laser from upper right of experimental cell, (B) chain involving dark and transparent particles without laser, (C) distinction of transparent particles by side of metal using laser in dark phase of microscope.

In fact, as we have discussed, the metal parallel to the field helped creating the maximum dipole, polarization mostly likely leading to assembly into the configuration with lowest energy projected here.

In order to verify this prediction of metal facing in transparent configuration, a red laser was used to shine light from the upper right or left side of the chamber. As the powerful laser has spatial coherence allowing it to be focused to a tight spot, it's used here to detect the metal placement. The transparent SU-8 allows transmission of laser, while the metal blocks and was bright red, from which we can tell the position of the metal. As demonstrated in Figure 12c, there was no light blocking occurred on the dark particles, because we were shining laser from left or right with regard to the image and the reflex wouldn't be seen through objective lens. But for the transparent ones, it's clear that metal of the first and fifth from above were on the right, while the middle three had their metal facing left. Illumination also helped checking whether all particles were assembled on the same plane. As might have been noticed, the last transparent particle tilted and didn't fully align with other particles (Figure 12c). Using the laser observation method, we examined transparent configuration over a large range of frequency (≥ 10 kHz) and voltage (≥ 50 V). The result definitely agreed with what we have predicted with modeling, where majority particles had metal facing the same side and minority were facing different sides parallel to the field direction.

For the dark chain orientation, laser wouldn't have helped much, as shining from the right top is not applicable and reflex wouldn't differ between metal on the top and on the bottom, unless SU-8 has low transparency. Instead, we managed to fabricate fluorescent particles based on the same method of photolithography and metal evaporation but adding fluorescent dye (2 mg Nile red / 1 mL SU-8) before spin-coating. The fluorescing method worked well for visualizing the metal side for dark configuration at low voltage. When the metal was on the bottom, particles flowed red, as the fluorescent parts of the SU-8 cubes were exposed to the objective. But compared with optical image, some particles 'disappeared' in fluorescence mode. That's because the non-fluorescent metal coating was on the top, blocking the fluorescent material underneath and resulting in appearing like dark background. Applying fluorescent particles for dark configuration at low voltage over a range of frequencies, we found that most particles assembled had their metal facet on the bottom and the minority with metal on the top would likely be isolated rather than aligned into chain, which was against our assumption that highly polarizable metal should be pulled upwards by the AC field in an

inverse cell due to positive dielectrophoresis exerted on it [31]. One possible explanation is that the initial particle distribution accounts for it to some extent. To verify this, we checked the ratio of particles with metal on the top against ones on the bottom using statistical methods. The results were convincing, since 3.5/1 bottom/top ratio clearly stated that it wouldn't be surprising if more dark particles stayed initially with metal on the bottom and the field with low voltage didn't provide enough energy to turn it over. Notably, these cubic particles are much larger and heavier than that of microspheres [7, 8, 31]. Moreover, once particles with metal on the bottom formed chains, it would be hard for the metal on the top to join, since the dipole-dipole interaction was not strong for metal on different planes. This natural sediment phenomenon is novel and hasn't been reported, and later on needs more attention and further investigation.

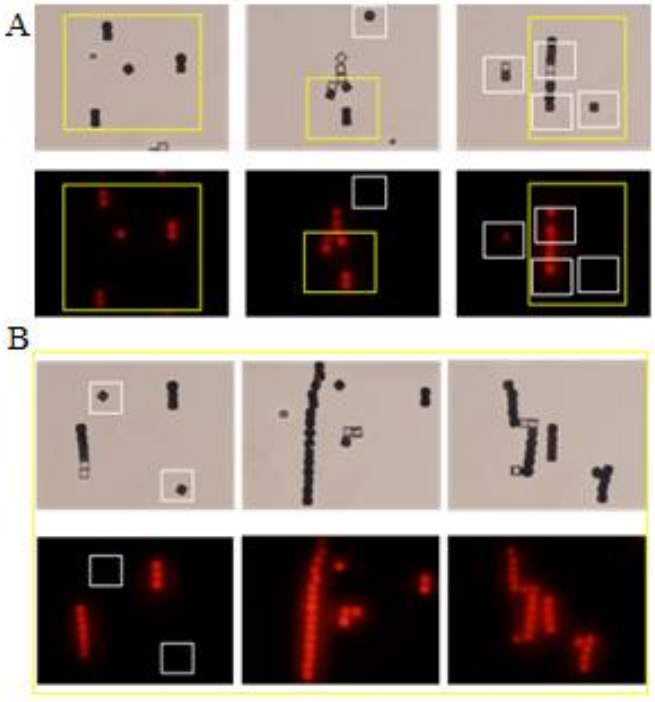

Figure 13. Discrimination between metal on the top and on the bottom for dark configurations using combination of optical and fluorescent microscopic images. Particles with metal on the top are circled by white while ones with metal on the bottom were circles with yellow squares. (A) 1 kHz and 31.90 V, (B) 20 kHz, 27.21 V.

In summary, the ‘quadrupolar’ interaction for one-side coated particles predominated at high voltage, while at low voltage and frequency dark configuration with interesting sedimentation process involved was against our assumption.

2.5 Summary and outlook

The one-side coated cubes have been explored using various methods, such as statistical distribution, laser illumination, and fluorescent imaging. Since we found that the distribution of particle configuration under various conditions was influenced by initial isolated particle distribution, using the calibration method mentioned in the paper, we need to represent the data in new way and obtain better understanding how they respond to the field.

Though the particle statics and kinetics were understood well with the help of COMSOL simulation at high frequencies, the simulation had limitation on investigating the 3D real environment of experiment where the field was non-uniform and real volume with cubic shape with each coordinate inside or outside experienced different field intensity and direction. Given the difficulties for studying the fundamental at low frequencies for dark orientation, we will continue on using fluorescent particles and clarify the relationship between configuration and sedimentation.

The one-sided coated cubes were also tested with magnetic field [31], forming zigzagged chains and elongated rods, which inspired our next step by including the magnetic field in addition to the electric field. We have obtained particles fabricated with two sides of metal coating where one was gold and the other was gold and nickel. Similar to the magnetic particles we used in assembling 2D responsive network, these particles respond both to the electric and the magnetic fields. The cubic shape would give them larger or smaller flexibility in assembling in two fields, which is surely going to be unique and fascinating.

Chapter 3
Assembling a 2D responsive colloidal network by combined electric and magnetic fields

3.1 Material and experimental setup

Two kinds of particles of similar size were used to form 2-D responsive network. Fluorescent green dielectric particles (Thermo Fisher Scientific Inc., MA) with 4.8 μm diameter only respond to AC electric field as other non-patch microspheres [6]. The 5.8 μm in diameter

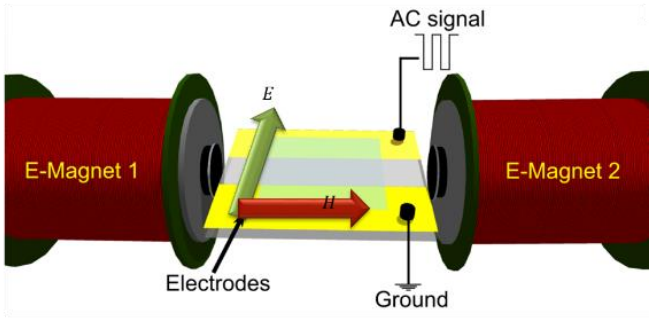

Figure 14. Schematics of 2-field assembly experimental setup where electric and magnetic field are exerted perpendicularly to each other.

latex particles with included iron in polymer matrix (Bangs Laboratories, Inc., IN) obey similar assembly rules in electric field but also respond to magnetic field because of their iron core. Both particles were cleaned with Milli-Q water with centrifuging and mixed before experiment.

The experimental setup (Figure 14) consisted of a glass slide with co-planner electrodes (2 mm gap in the middle), same with slide for previous studies [6-8]. Two spiral coils connecting DC electric signal were placed symmetrically at each end of the gap, so that the

axles of coils aligned along the middle and stayed at the same height of the experimental cell. An imaging spacer with 20 mm diameter and 0.12 mm depth (Electron Microscopy Sciences,) containing particle suspension was placed onto the electrodes. AC signal (10 kHz, 0 – 100 V) was applied to the electrodes, and magnetic fields was on when DC current (1 – 20 V, 0.1 – 5 A) was passed through the coil. The experimental setup was capable of applying electric and magnetic field perpendicular to each other on the same plane where colloidal assembly went on. Two switches were used to control the AC and DC signal separately, so that the order of turning on field could be designed.

3.2 Study of 2D percolation process

With same number density of two particles, 2-dimensional chaining grew when both fields were on, and the rate depends on the intensities of the fields. As particle alignment went on at one specific direction, there was no way to avoid encountering chain in other direction, if the number density was high enough. During the meeting of chains in perpendicular directions, the magnetically responsive particles in horizontal direction acted like point or part of chain

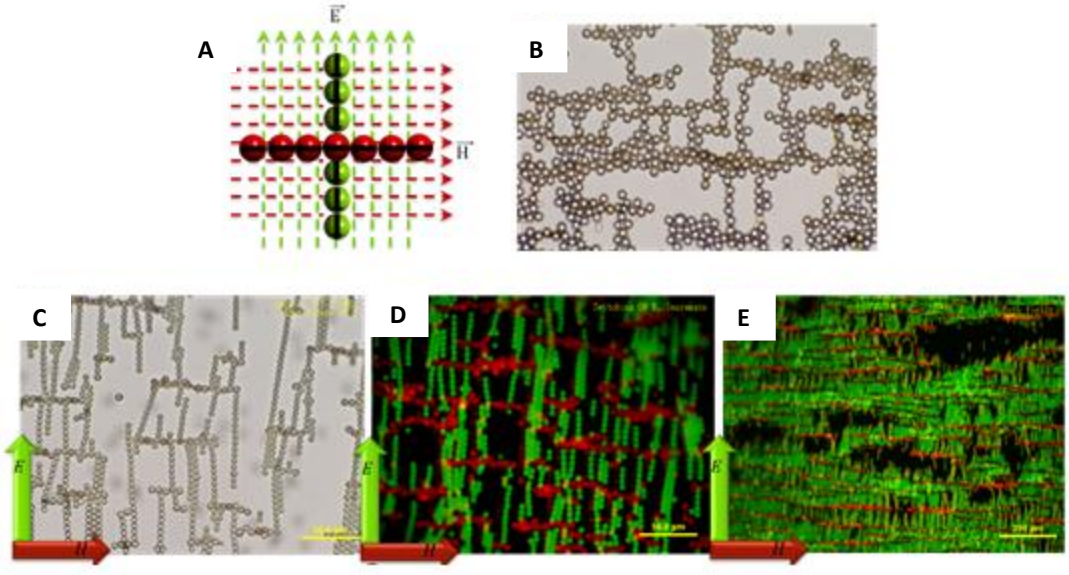

Figure 15. 2D percolated network. (A) chaining of fluorescent particles along the field respectively, (B) equilibrium state achieved at H = 700 A/m and E = 10 kHz, 12 V/mm, (C) optical microscopic image of 2D percolation, (D) fluorescent view of percolation, (E) fully percolated particle system in a larger view using small magnification of objective.

intersection and connected two chains, because they responded not only to the magnetic field but also to the electric field and stayed stable as part of dielectric and magnetic alignment. With time, the horizontal and vertical chains got intersected more and more, leading to 2D percolation. After certain period of time depending on the field intensities (< 10 min), the networking process proceeded much slower and approached its equilibrium state, such that the well percolated colloidal assembly formed with fully connectivity in both vertical and horizontal directions and highly condensed junctions. Four parameters we observed so far played important roles determining the structure of 2-D percolated network, including particle number density, ratio of two kinds of particles, intensity of electric and magnetic fields.

For now, to investigate the fundamental of mechanism of system, we kept the ratio (1:1) and number density constant to simply the study. Here's an example (Figure 15), under certain condition of magnetic and electric field intensity, highly cross-linked, fully percolated structure formed under two fields perpendicular to each other. By increasing the intensity of the electric field, the shape of the 2D colloidal network transformed to state where area of interspace units created by four adjacent particle chains were enlarged, resulting from higher rate of assembly in the vertical direction before being intersected. It is much clear from the fluorescent image how particles percolated as the red magnetic microspheres aligned horizontally and connected the green dielectric particles in vertical direction. A broader view of the percolation (Figure 15) convinced us that it has the ability to achieve a uniform and well percolated 2D network covering flat surface, which provides potential for industrial reproduction in large scale.

3.3 Two different mechanism of assembly

In our study, we managed to manipulate two kinds of particles to form 2D percolated network by two different mechanisms. The resulting distinction was dependent on the nature of the magnetic particles. As mentioned above, the magnetic particles were produced by adding iron component into latex microsphere matrix, offering their capability of being induced by both AC electric and magnetic fields. Turning on either of fields, the magnetic

particles could form chains in the direction of field, which means with only magnetic particles in the system electric and magnetic fields competed for the particle alignment based

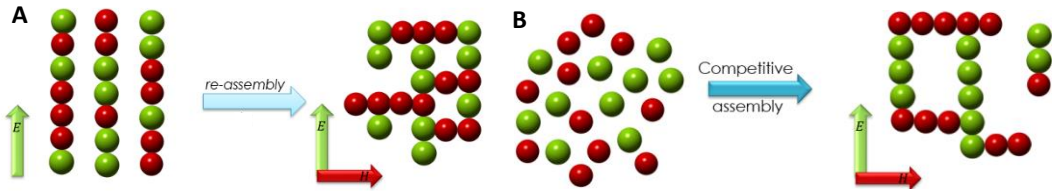

Figure 16. Two mechanism of assembly with two fields. (A) re-assembly by electric then magnetic field, (B) competitive assembly by two fields at the same time.

on the intensities. The magnetic particles then could also form 2D network on their own, and adjusting the intensities of two fields would provide flexibility of transformation among various percolated structure. However, from the perspective of material application, it is more interesting if we can assemble 2D percolated networks showing anisotropic properties such as electric or magnetic conductivity.

The two different mechanism were named ‘re-assembly’ (sequential assembly) and ‘competitive assembly’ (simultaneous assembly). The sequential assembly took advantage of the bi-responsive characteristics of magnetic particles, and was achieved by turning on AC electric field first and magnetic field later. When DEP was carried out, all particles formed chains vertically regardless of what type they were. Magnetic and dielectric particles in these vertical chains were in random sequence independent of small difference in polarizability, which related to size and modification of particles. After formation and equilibrium of long vertical alignment, magnetic field with intensity large enough compared to the electric field came in. Once the magnetic field was turned on, magnetic particles started to re-arrange themselves to align in horizontal direction and connect the modified vertical chains. The equilibrium was established and 2D percolation was achieved by turning on fields sequentially.

In contrast to sequential assembly, the simultaneous assembly worked faster under same condition by switching on two fields at the same time in the beginning. The dielectric

particles surely assembled into vertical chains, while there was competition between magnetic and electric fields for the bi-responsive magnetic particles. By adjustment of relative field intensities, we were able to align more magnetic particles in horizontal direction and percolate the 2D chains as in Figure 16.

Both mechanism worked differently but well for succeeding in formation of 2D bi-responsive colloidal network.

3.4 Kinetics study of particle networking

To understand the two mechanism from the perspective of fundamental principle, we employed again the statistical method for kinetic analysis. For each of the two mechanism, we chose experiments done in the same condition and analyzed by counting the number of

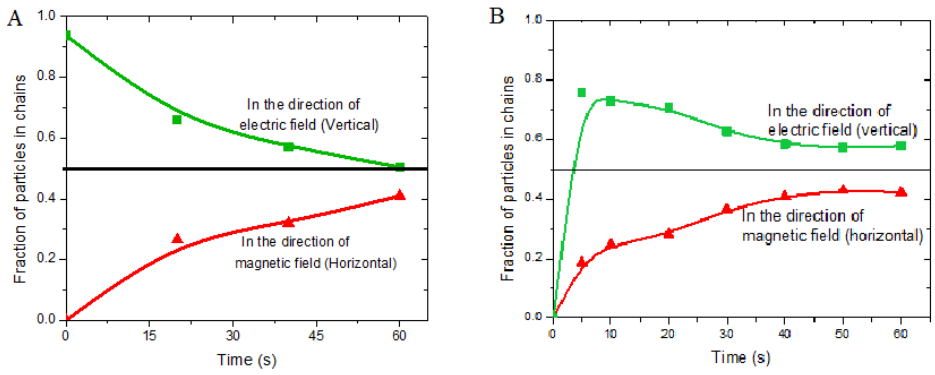

Figure 17. Fraction of particles in chains versus time in direction of fields respectively. (A) re-assembly, (B) competitive assembly.

particles in chains (vertical and horizontal) respectively at increasing time point. Calculation of percentage of particles involved in either direction (Figure 17) illustrated how particles assembled with regard to time. It's not surprising that the 're-assembly' process resulted in almost all particles aligned in vertical direction and magnetic field later on took out bi-responsive magnetic particles inserted and forced them in horizontal chaining. With time going, number of particles in each direction equaled, which was also true with 'competitive assembly'. However, the assembly rate determined by the slope of curve at small times was

different for two chain direction, as the vertical chains grew faster than the horizontal ones. This inspired us to suggest a concept how to formulate the 2D network with lowest density but largest porosity. If we could adjust the field intensities in a way to equal the growing rate of particle chaining in each direction, given constant number of particles with 1:1 particle ratio, the square interspace within percolation would be large. Over a confined area, the density of particles would be lowest. However, more experiments and further study are required to verify this hypothesis.

3.5 Characterization by programming

Software processing was also used to analyze the percolated network, for its convenience, accuracy and additional informational function. ImageJ^{TM} and SciLab^{TM} were combined to realize the goal. In ImageJ^{TM}, data for each particle were collected after pretreatment of the microscopic image, especially the pixel coordinate (x, y). A big matrix with more than 500

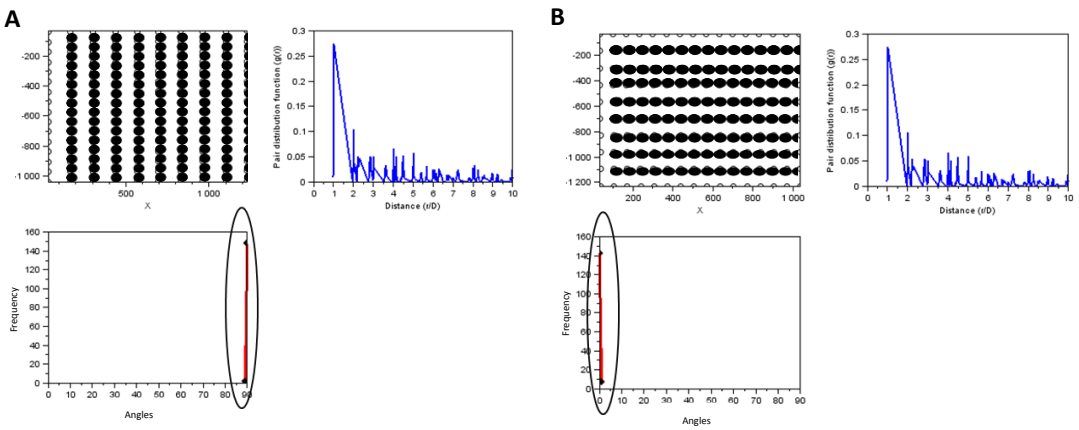

Figure 18. Software output of chaining in two specific direction. (A) vertical chains, (B) horizontal chains.

rows of coordinate information was then input into the coding we coded with SciLab^{TM}, whose output includes pair distribution function and distribution of angle with adjacent particles [29, 30]. To check whether it worked precisely, we drew two images ourselves, one with all alignment in the vertical direction and other had only horizontal chains. These two cased were process with steps mentioned above and results are shown in Figure 18. Indicated by the distribution of angle which represented the direction of alignment, all particles in both

cased were definitely at the same angle but different value, where 90^0 showed vertical alignment and 0^0 meant horizontal connection. The pair distribution function was used to calculate all the possible distance between each pair of particles, which was determined using the relation

$$g(r) = \frac{\delta N}{2\pi r \delta r} \qquad (12)$$

Where r is distance between particles, δr is the increment in r, δN is the number of particles in the distance range δr. Initially, all the distances were in the units of pixels. [33] Normalized distances r/D were obtained by dividing the distances with average particle diameter (in pixels). In both cases, the results showed a distinct maximum at a pair distance equal to the diameter of the particle (r/D= 1) and further weak maximum at a pair distance of integer number (2, 3, 4…), indicating the formation of linear chains. Output of these two cases was in perfect agreement with what we could observe clearly from the images designed, which showed the liability of the method. Thus, we now have the tools to better understand the system and characterize it more precisely.

3.6 Summary and outlook

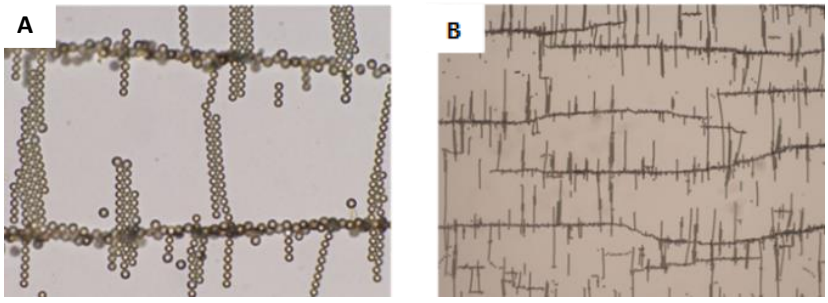

Figure 19. Percolation with lowest number density achieved at 2.76 A and 48 V. (A) optical image with 50X magnification objective, (B) image with 10X magnification.

We have developed technique to understand better the kinetics and equilibrium 2D structures, though more experiments and application of technique need to be performed. Deeper exploration towards the fundamental is required for simple system with similar size

and fixed ratio of particles, and further investigation of the effect of the conditions will be needed. The optimalization should be continued for identifying proper cases of low density and high porosity percolation.

In addition, it would be interesting to show the structure assembled corresponding to the intensities of fields in a phase diagram, just like Janus particles [8], to give a better macroscopic view of what kind of percolation we can achieve and their potential application.

References

1. Velev O.D.; Jede T.A.; Lobe R.F.; Lenhoff A.M. “Porous silica via colloidal crystallization” *Nature* **1997**, 389, 447–448
2. Joannoupolous, J. D.; Meade, R. D.; Winn, J. N. *Photonic Crystals*; Princeton University Press: New Jersey, **1995**
3. Yablonovitch, E. “Inhibited Spontaneous Emission in Solid-State Physics and Electronics” *Phys. Rev. Lett.* **1987**, *58*, 2059-2062.
4. Velev O. D.; Kaler E. W. “In Situ Assembly of Colloidal Particles into Miniaturized Biosensors” *Langmuir* **1999**, 15 (11), 3693–3698
5. Velev,O. D.; Gupta, S. “Materials Fabricated by Micro- and Nanoparticle Assembly - The Challenging Path from Science to Engineering” *Adv. Mater.* **2009**, 21, 1897
6. Lumsdon, S. O.; Kaler, E. W.; Velev,O. D. “Two-dimensional Crystallization of Microspheres by a Coplanar AC Electric Field” *Langmuir* **2004**, 20, 2108
7. Velev, O. D.; Bhatt, K. H. “On-chip Micromanipulation and Assembly of Colloidal Particles by Electric Fields” *Soft Matter* **2006**, 2, 738–750
8. Gangwal, S.; Cayre, O. J.; Velev, O. D. “Dielectrophoretic Assembly of Metallodielectric Janus Particles in AC Electric Fields” *Langmuir* **2008**, 23, 13312–13320.
9. Kretzschmar, I.; Song, J.H. “Surface-Anisotropic Spherical Colloids in Geometric and Field Confinement” *Curr. Opin. Colloid Interface Sci.* **2011**, 16, 84–95.
10. Evers, W. H., et al. "Entropy-driven formation of binary semiconductor-nanocrystal superlattices" *Nano letters.* **2010**, 10, 4235-4241.
11. Denkov, N. D., et al. "Mechanism of formation of two-dimensional crystals from latex particles on substrates" *Langmuir*, **1992**, 8, 3183-3190.
12. Denkov, N. D., et al. "Two-dimensional crystallization" *Nature*, **1993**, 361, 26.
13. Singh, Gurvinder, et al. "Multicomponent colloidal crystals that are tunable over large areas." *Soft Matter*, **2011**, 7, 3290.

14. Singh, Gurvinder, et al. "Highly Ordered Nanometer-Scale Chemical and Protein Patterns by Binary Colloidal Crystal Lithography Combined with Plasma Polymerization." *Adv. Funct. Mater.*, **2011**, 21, 540-546.
15. Dimitrov, A. S.; Takahashi, T.; Furusawa, K.; Nagayama, K. "Two-dimensional Patterns of Magnetic Particles at Air-Water or Glass-Water Interfaces Induced by an External Magnetic Field: Experimental Observation and Dependencies" *J. Phys. Chem.* **1996**, 100, 3163–3168.
16. Velev,O. D.; Gangwal, S.; Petsev, N. D. "Particle-localized AC and DC manipulation and electrokinetics" *Annu. Rep. Prog. Chem., Sect. C*, **2009**, 105, 213–246
17. Jones, T. B. *Electromechanics of Particles*; Cambridge University Press: Cambridge, **1995**
18. Pohl, H. A. *Dielectrophoresis*; Cambridge University Press: Cambridge, **1978**
19. Morgan, H.; Green, N. G. *AC Electrokinetics: colloids and nanoparticles*; Research Studies Press Ltd.: Hertfordshire, UK, **2003**
20. Gangwal S., Pawar A. B., Kretzschmar I., Velev O. D. "Programmed Assembly of Metallodielectric Patchy Particles in External AC Electric Fields" *Soft Matter*, **2010**, 6, 1413 – 1418
21. Velev, O. D.; Lenhoff, A. M.; Kaler, E. W. "A Class of Microstructured Particles through Colloidal Crystallization" *Science*, **2000**, 287, 2240–2243
22. Cayre, O.; Paunov, V. N.; Velev, O. D. "Fabrication of Asymmetrically Coated Colloid Particles by Microcontact Printing Techniques" *J. Mater. Chem.*, **2003**, 13, 2445–2450
23. Love, J. C.; Gates, B. D.; Wolfe, D. B.; Paul, K. P.; Whitesides, G. M. "Fabrication and Wetting Properties of Metallic Half-shells with Submicron Diameters" *Nano Lett.*, **2002**, 2, 891–894
24. Herlihy, K. P.; Nunes, J. and DeSimone J. M. "Electrically driven alignment and crystallization of unique anisotropic polymer particles" *Langmuir*, **2008**, 24, 8421-8426.
25. Erb, R. M., et al. "Magnetic assembly of colloidal superstructures with multipole symmetry" *Nature*, **2009**, 457, 999-1002.

26. Ahniyaz, A.; Sakamoto, Y. and Bergstrom, L. "Magnetic field-induced assembly of oriented superlattices from maghemite nanocubes" *Proc. Natl. Acad. Sci. U. S. A.*, **2007**, 104, 17570-17574.
27. Yang, Y. R.; et al. "Imaginary Magnetic Tweezers for Massively Parallel Surface Adhesion Spectroscopy" *Nano Lett.*, **2011**, 11, 1681-1684.
28. Erb, R. M.; et al. "Towards holonomic control of Janus particles in optomagnetic traps" *Adv. Mater.*, **2009**, 21, 4825-4829.
29. Corsi, A. and Gujrati, P. D.. "Percolation of particles on recursive lattices using a nanoscale approach. III. Percolation of polydisperse particles in the presence of a polymer matrix" *Physical Review*, **2006**, 74, 061123.
30. Bouvard, D. and Lange, F. F. "Relation between percolation and particle coordination in binary powder mixtures." *Acta metallurgica et materialia*, **1991**, 39, 3083-3090.
31. Shields, C.; et al. "Field-directed assembly of patchy anisotropic microparticles with defined shape." *Soft Matter*, **2013**.
32. Gangwal, S.; et al. "Induced-charge electrophoresis of metallodielectric particles." *Physical review letters*, **2008**, 100, 058302.
33. Bharti, B., Meissner J. and Findenegg, G. H. "Aggregation of silica nanoparticles directed by adsorption of lysozyme." *Langmuir*, **2011**, 27, 9823-9833.